Electronic Supplementary Material (ESI) for Journal of Materials Chemistry A.

Enhanced visible-light-driven hydrogen generation by *in situ* formed photocatalyst RGO-CdS-Ni_xS from metal salts and RGO-CdS composites

Jiu-Ju Wang, Jing Wang, Ke Feng,* Hui-Hui Zhang, Zhi-Jun Li, Bin Liu, Chen-Ho Tung and Li-Zhu Wu*

Key Laboratory of Photochemical Conversion and Optoelectronic Materials, Technical Institute of Physics and Chemistry & University of Chinese Academy of Sciences, Chinese Academy of Sciences, Beijing 100190, P. R. China.

E-mail: kefeng@mail.ipc.ac.cn, lzwu@mail.ipc.ac.cn.

Supporting information

Table of Contents

1. Synthesis.

The synthesis of $(RGO)_n$-CdS composites are based on a modified method reported by Cao *et al.*[1] In brief, GO with the desired weight proportion was firstly dispersed in DMSO by ultrasonication and prepared a homogeneous solution. To a 40 mL of the above solution, 0.106 g $Cd(CH_3COO)_2 \cdot 2H_2O$ was added , the mixture was stirred vigorously and transferred to a 50 mL Teflon-lined autoclave, after held at 180°C for 12 h, the formed precipitates from the mixture were allowed to be collected by centrifugation, and then rinsed with acetone and ethanol to remove DMSO residue. The obtained product was dried in an oven at 60°C for 12 h. The weight ratios of GO to $Cd(CH_3COO)_2 \cdot 2H_2O$ were 0%, 0.5%, 1.0%, 2.0%, 4.0% and 7.0%, and the obtained samples were labeled as $(RGO)_0$-CdS, $(RGO)_{0.5}$-CdS, $(RGO)_{1.0}$-CdS, $(RGO)_2$-CdS, $(RGO)_4$-CdS, and $(RGO)_7$-CdS, respectively.

2. Figure S1.

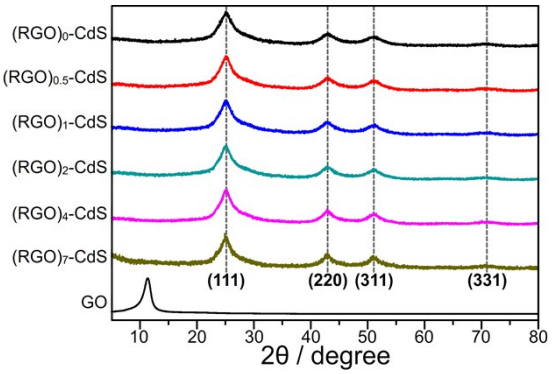

Figure S1. XRD patterns of GO and $(RGO)_n$-CdS (n = 0, 0.5, 1, 2, 4 and 7).

3. Figure S2.

ATR FT-IR spectra provided a qualitative measurement of the deoxygenating reaction. For GO, a broad, intense band at 1728 cm^{-1} (C=O stretching vibrations from carbonyl and carboxyl groups), 1622 cm^{-1} (C=C stretching, skeletal vibrations from unoxidized graphitic domains), 1409 cm^{-1} (O-H bending vibrations from hydroxyl groups), 1215 cm^{-1} (C-OH stretching vibrations), and the bands at 1050 cm^{-1}, however, implied a certain fraction of epoxy or ether functionalities remained.

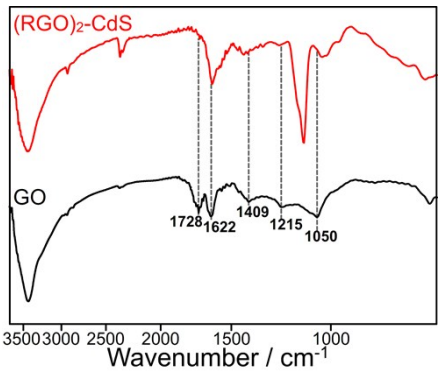

Figure S2. ATR FT-IR spectra for GO and $(RGO)_2$-CdS.

4. Figure S3.

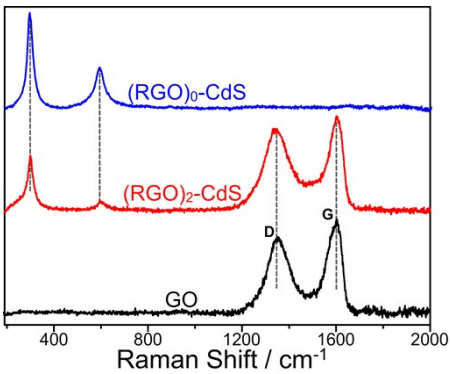

Figure S3. Raman analysis of $(RGO)_0$-CdS, $(RGO)_2$-CdS and GO.

5. Figure S4.

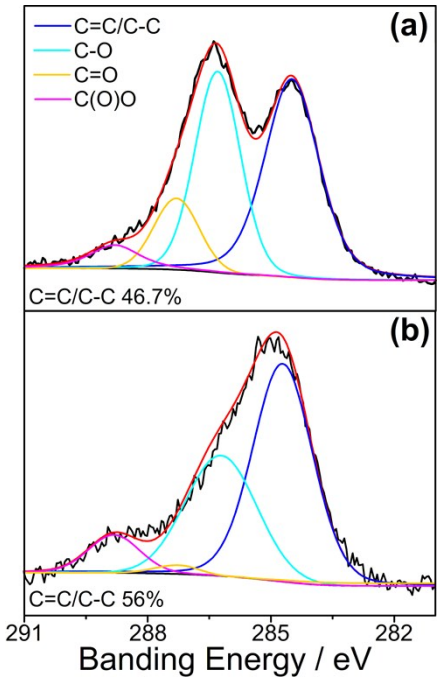

Figure S4. C 1s XPS spectra of GO (a) and $(RGO)_2$-CdS (b).

When the contributing peak areas were analyzed, the relative content of carbon in the RGO_2-CdS sample by the following equation[2] is up to 56%, comparable to the value of 46.7% for GO,

$$\%(C=C/C-C)=\frac{A_{C=C/C-C}}{A_{C=C/C-C}+A_{C-O}+A_{C=O}+A_{C(O)O}}$$

where $A_{C=C/C-C}$, $A_{C=O}$, A_{C-O} and $A_{C(O)O}$ are the peak areas for graphitic (C=C/C-C) and O-bound related (C=O, C-O and ester bond) carbon, respectively.

6. Figure S5.

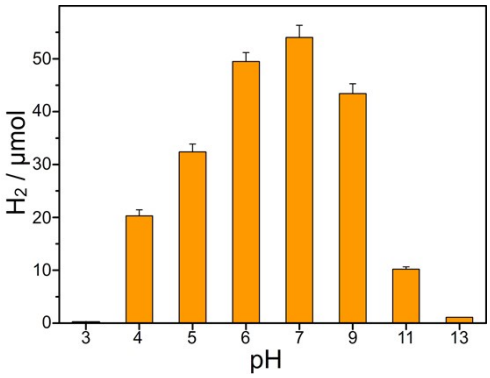

Figure S5. Visible-light-driven H_2 production activity of $(RGO)_2$-CdS at varied pH. Measurement conditions: 0.5 mg photocatalysts with Ni^{2+} (2.1×10^{-4} M) in 10 mL ethanol/water (*v*/*v*, 1/1) solution, $\lambda > 400$ nm, 6 h.

7. Figure S6.

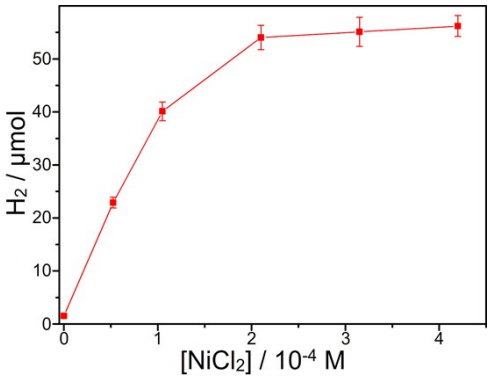

Figure S6. Visible-light-driven H_2 production activity of $(RGO)_2$-CdS with varied concentration of $NiCl_2$. Measurement conditions: 0.5 mg photocatalysts in 10 mL ethanol/water (*v*/*v*, 1/1) solution, pH 7, $\lambda > 400$ nm, 6 h. Considering the total amount, turnover number and turnover frequency during photocatalytic H_2 evolution, the optimized [$NiCl_2$] was determined as 2.1×10^{-4} M.

8. **Figure S7.**

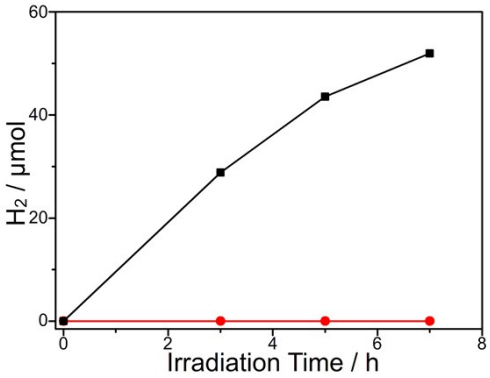

Figure S7. H_2 reproducable activity for the precipitates (black) and the colourless up-solution (red), obtained from the H_2 photoproduction system containing $(RGO)_2$-CdS and Ni^{2+} after the visible-light irradiation ($\lambda > 400$ nm).

9. **Figure S8.**

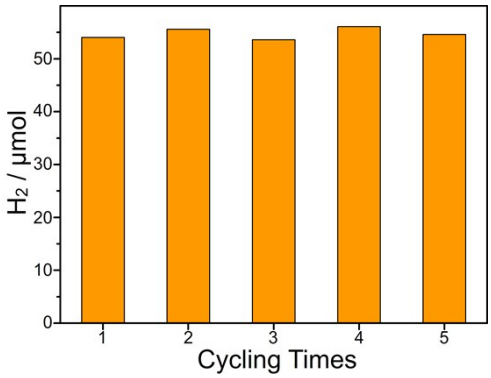

Figure S8. Cycling test of H_2 producable activity for $(RGO)_2$-CdS-Ni_xS at pH 7 with the visible light irradiation ($\lambda > 400$ nm) for 6 h.

10. **Figure S9.**

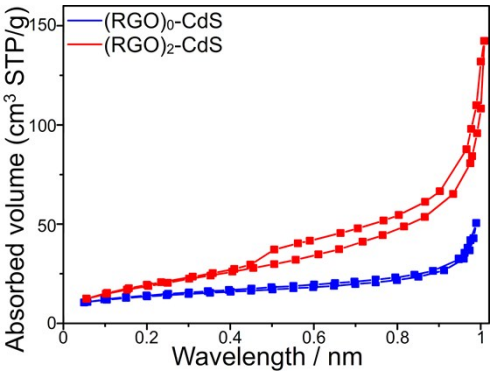

Figure S9. Nitrogen absorption isotherms of $(RGO)_0$-CdS and $(RGO)_2$-CdS.

11. Figure S10

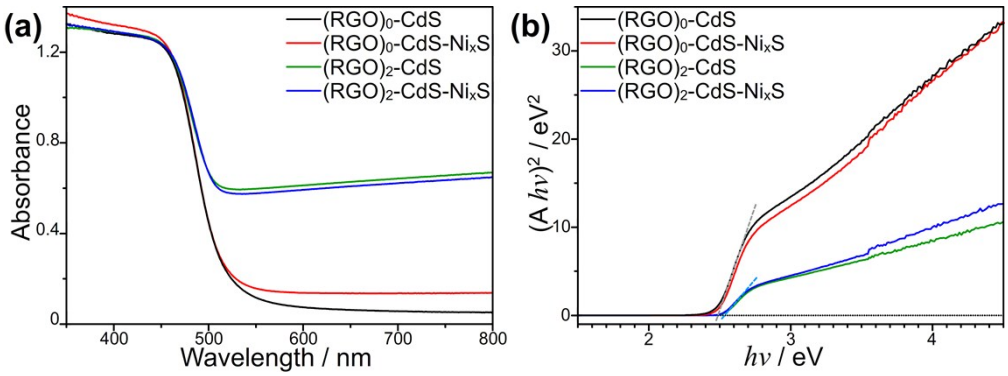

Figure S10. DRS spectra (a) and E_g calculation (b) of $(RGO)_0$-CdS, $(RGO)_2$-CdS, $(RGO)_0$-CdS-Ni_xS and $(RGO)_2$-CdS-Ni_xS.

12. Figure S11.

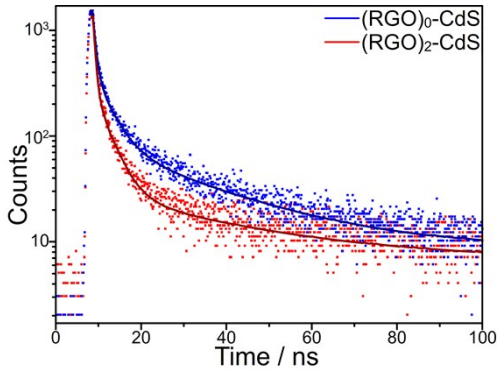

Figure S11. Time resolved photo-emission decay profiles of $(RGO)_0$-CdS (τ = 10.1 s) and $(RGO)_2$-CdS (τ = 8.16 s). Excitation for the samples were fixed at 406 nm, and the emission profiles were monitored at 550 nm. The solid lines represent the best fits obtained by deconvolution.

13. Figure S12.

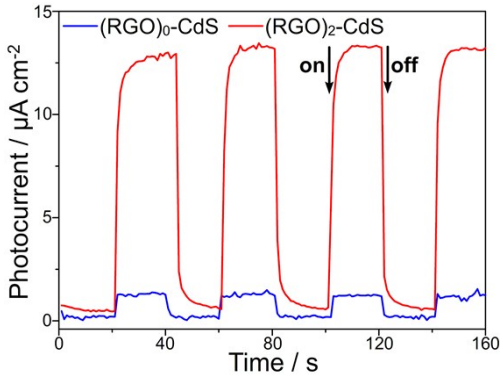

Figure S12. Transient photocurrent response of $(RGO)_0$-CdS (black) and $(RGO)_2$-CdS (red) composites on FTO conductor glass in 0.5 M Na_2SO_4 aqueous solution with bias of 0.2 V (*vs* Ag/AgCl) under the visible-light

irradiation (λ > 400 nm).

14. Scheme S1.

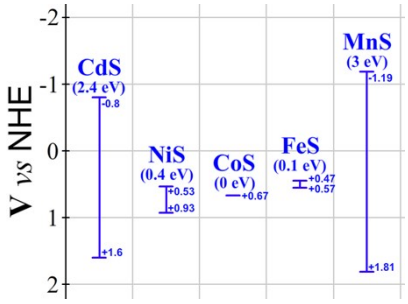

Semiconductor	E_g (eV)[3]	E_{CB} (V *vs.* NHE)	E_{VB} (V *vs.* NHE)
NiS	0.40	0.53	0.93
CoS	0	0.67	0.67
FeS	0.10	0.47	0.57
MnS	3.00	-1.19	1.81

Scheme S1. Comparison of the conduction and valence bands for CdS, NiS, CoS, FeS and MnS.

15. Figure S13.

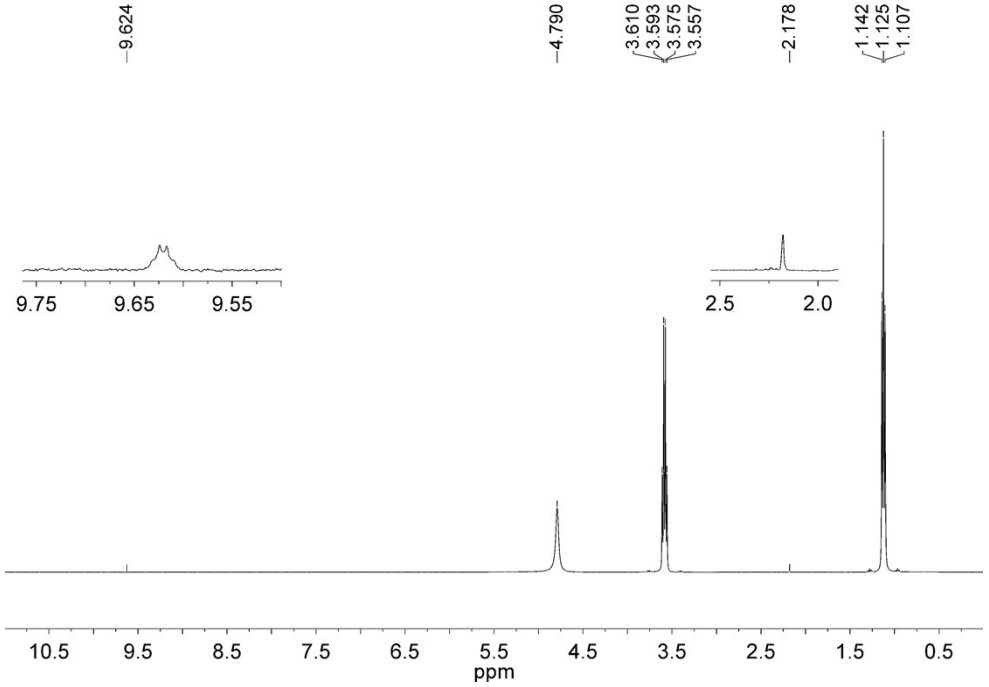

Figure S13. ^{1}H-NMR spectrum for the product obtained during photocatalytic H_2 generation. A new peak at 9.62 ppm corresponding to the aldehyde group resonance in acetaldehyde and a new peak at 2.18 ppm corresponding to the methyl group resonance in acetaldehyde.

16. Figure S14.

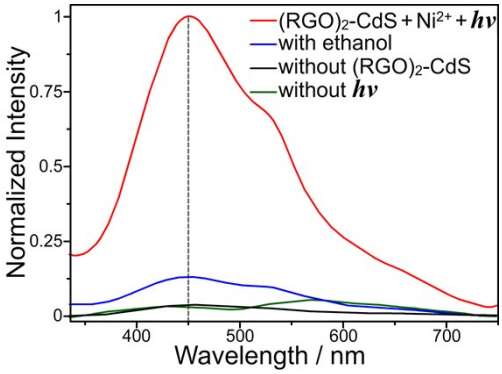

Figure S14. ·OH trapping fluorescence spectra of in the reaction systems with the addition of TANa: (red) $(RGO)_2$-CdS (0.5 mg), $NiCl_2 \cdot 6H_2O$ (2.1×10^{-4} M) in aqueous solution at pH 7 with the visible light irradiation ($\lambda >$ 400 nm) for 20 min; (blue) the system is the same as (red) except that ethanol was added; (black) the system is the same as (red) except that $(RGO)_2$-CdS was absent; (green) the system is the same as (red) but the solution was kept in dark for 20 min. The concentration of TANa was 5.0×10^{-3} M throughout the experiments, excitation wavelength at 312 nm.

17. References.

1. A. Cao, Z. Liu, S. Chu, M. Wu, Z. Ye, Z. Cai, Y. Chang, S. Wang, Q. Gong and Y. Liu, *Adv. Mater.*, 2010, **22**, 103-106.
2. A. Iwase, Y. H. Ng, Y. Ishiguro, A. Kudo and R. Amal, *J. Am. Chem. Soc.*, 2011, **133**, 11054-11057.
3. Yong Xu and Martin A. A. Schoonena, *American Mineralogist*, 2000, **85**, 543-556